

iCub Detecting Gazed Objects: A Pipeline Estimating Human Attention

Shiva Hanifi¹, Elisa Maiettini^{1†}, Maria Lombardi^{1†} and Lorenzo Natale¹

Abstract—This paper explores the role of eye gaze in human-robot interactions and proposes a novel system for detecting objects gazed by the human using solely visual feedback. The system leverages on face detection, human attention prediction, and online object detection, and it allows the robot to perceive and interpret human gaze accurately, paving the way for establishing joint attention with human partners. Additionally, a novel dataset collected with the humanoid robot iCub is introduced, comprising over 22,000 images from ten participants gazing at different annotated objects. This dataset serves as a benchmark for evaluating the performance of the proposed pipeline. The paper also includes an experimental analysis of the pipeline’s effectiveness in a human-robot interaction setting, examining the performance of each component. Furthermore, the developed system is deployed on the humanoid robot iCub, and a supplementary video showcases its functionality. The results demonstrate the potential of the proposed approach to enhance social awareness and responsiveness in social robotics, as well as improve assistance and support in collaborative scenarios, promoting efficient human-robot collaboration. The code and the collected dataset will be released upon acceptance.

I. INTRODUCTION

Any face-to-face interaction between two people is characterised by a continuous exchanging of social signals, such as gaze, gestures, facial expression and so on. Such kind of non-verbal communication is possible because both interacting individuals are able to see each other, perceive and understand the social information enclosed in such cues. In this paper, we focus on one of the most crucial social cue, that is the eye gaze. Eye gaze plays a pivotal role in many mechanisms of social cognition, e.g. joint attention, in regulating and monitoring turn taking, signalling attention and intention. Much neuropsychological evidences highlighted the close relationship between gaze direction and attention, indicating that gaze functions are actively involved and influenced by spatial attention systems [1], [2]. For example, it is more likely that the gaze is directed toward an object rather than toward empty space.

In this context, the ability of a robot to determine what the human is looking at (e.g., an object) has numerous practical implications across various domains. In social robotics, it

*This work received funding by the Italian National Institute for Insurance against Accidents at Work (INAIL) ergoCub Project, the project Fit for Medical Robotics (Fit4MedRob) - PNRR MUR Cod. PNC0000007 - CUP: B53C22006960001 and Future Artificial Intelligence Research (FAIR) – PNRR MUR Cod. PE0000013 - CUP: E63C22001940006.

†These authors contributed equally to the work

¹Shiva Hanifi, Elisa Maiettini, Maria Lombardi and Lorenzo Natale are with Humanoid, Sensing and Perception Group, Istituto Italiano di Tecnologia, Genoa, Italy. shiva.hanifi@iit.it, elisa.maiettini@iit.it, maria.lombardi1@iit.it lorenzo.natale@iit.it



Fig. 1: *ObjectAttention* dataset: data collection setup with 6 objects from the YCB dataset [6] placed on a table between a human partner and iCub. Objects from left to right: *Driller*, *Bleach*, *Sugarbox*, *Mustard*, *MasterChef*, *Pringles*

can enhance the robot’s social awareness and responsiveness, allowing it to engage in more natural and contextually appropriate interactions [3], [4]. For instance, a robot capable of recognizing the object a human is looking at can infer the person’s preferences and tailor its actions or suggestions accordingly, thereby fostering personalized and adaptive experiences. Moreover, in collaborative scenarios, such as industrial settings or domestic environments, the robot’s capacity to understand human attention can significantly improve its ability to assist and support humans [5]. By detecting the objects that humans focus on during a task, the robot can anticipate their needs, provide relevant information, or even proactively offer assistance, thereby streamlining workflow and promoting efficient human-robot collaboration.

In this paper, we present a novel application for human-robot interaction that leverages computer vision techniques to enable robots to detect the object the human partner is gazing at. Our proposed system combines an online object detection algorithm [7], [8] with gaze tracking technologies, providing the robot with online information about the objects that capture the human’s attention. This integration offers a valuable cognitive capability for the robot, empowering it to perceive and interpret the human gaze within its environment accurately. That can be the first step to make the robot able to establish a conscious joint attention with the human partner [9].

The contribution of this work are as follows:

- We propose a pipeline to detect the target of human attention during an interaction with a robot. This pipeline leverages on a face detection, a human attention

prediction, and an online object detection to detect the object that the human focuses on.

- We present the ObjectAttention dataset collected with the humanoid robot iCub [10] where 10 participants gaze at different objects placed randomly on a table in front of the robot, totalling an amount of over 22K images. This dataset serves as a benchmark for application performance evaluation.
- We perform an experimental analysis of the proposed pipeline to evaluate its effectiveness in the considered HRI setting. For doing that we use the collected dataset and we study the performance of the components of the entire system.
- Finally, we deploy the system on the humanoid robot iCub. The video submitted as supplementary material shows the functioning of the developed system.

The rest of the paper is organised as follows. In Sec. II, we overview the state of art on robots having social skills and on HRI-based learning pipeline. The proposed architecture and the collected dataset are described in Sec. III and in Sec. IV, respectively. Sec. V reports the results obtained in our experimental analysis. Finally, in Sec. VI we conclude the paper.

II. RELATED WORK

The problem of endowing robot with the ability to understand human behaviour and specifically the social cue of the gaze has been largely studied in the literature. It is mainly addressed following two different strategies: 1) gaze estimation (i.e. estimating the gaze vector or mutual gaze events) and 2) gaze attention prediction (i.e. understand where the human is visually attending in terms of saliency map).

Following the *gaze estimation strategy*, a learning architecture to detect events of mutual gaze was proposed in [11]. This study emphasized the importance of mutual eye contact as crucial social cue in face-to-face interactions since it can be a signal of the readiness and attention of the interacting partner. In addition to the detection of mutual gaze events, several works focused on the estimation of the human gaze as a 2D or 3D vector. In [12] a feed-forward convolutional neural network was used to extract features from the RGB image (face image, right and left eye images) and produce as output the (x,y) coordinate of the gaze prediction. The use of the CNN architecture to estimate the 2D gaze vector is also proposed in [13], but with the novelty to extract features from only one eye. Strength of such an One-eye Gaze estimation approach is that in real worlds conditions it is very common that the human face and/or their eyes are partially obscured (i.e. in this case the two-eyes models would probably fail). An example of predicting 3D gaze vector can be found in [14]. The authors proposed a combination of a regression network (FAR-net) and an evaluation network (E-Net) able to exploit the asymmetry and the difference between left and right eyes.

Much effort has been spent in building *attention architectures* that, for example, enable joint attention between

a human and the humanoid robot iCub with the aim to improve the performance of visual learning methods [15]. Another example is in [16] where the authors proposed a method, called Attention Flow, to learn joint attention in an end-to-end fashion by employing saliency-augmented attention maps and two innovative convolutional attention mechanisms that choose important cues and improve joint attention localization. Moreover, in [17], a spatial-temporal neural network (LSTM network) was proposed to detect shared attention intervals in third-person social videos and predict shared attention locations in frames.

The problem of the gaze following was addressed, instead, in [18] and [19]. The former used a CNN architecture that leverages the geometry of the scene. Specifically, it takes as input the RGB frame (with the person's head location and the eye coordinates within that frame) and a set of neighboring frames from the same video and identifies which of the neighboring frames, if any, contain the object being looked at and the coordinates of the person's gaze. The latter proposed a two-stage solution for gaze following. In the first stage, which is a gaze direction pathway, it takes as an input the head image and the head position and generates multi-scale gaze direction fields by using ResNet-50 as features extractor. In the second stage, which is a heatmap pathway, the framework tries to infer the gaze point taking into account the gaze direction and the context information of the objects along the gaze direction.

Despite gaze estimation and human attention have been largely studied, very few works exist that combine the estimation of the human attention with the prediction of the target object. Among these few, authors in [20] proposed an approach to predict human referential gaze having both the person and object of attention visible in the image. The proposed network contains two pathways: one for estimating the head direction and another for salient objects in the image. Such a work was used as backbone in [21] and extended in order to address out-of-frame gaze targets by simultaneously learning gaze angle and saliency. Moreover, differently from [20], an LSTM-based spatio-temporal model is used to leverage on the temporal coherence of the frames in videos to improve gaze direction estimation. However, in [21], only the gaze direction of the human is predicted, while the information of the target object is not provided.

In this paper, we exploit the LSTM-based spatio-temporal model presented in [21] and we adapt it to the considered HRI setting by fine-tuning it on the proposed ObjectAttention dataset. Moreover, we use it in conjunction with a human pose estimation and a face detector to make the pipeline run online on the humanoid robot iCub. Finally, by integrating an online object detection method, we allow the system to predict the class label and location of the gaze target object. Note that, differently from [20], by using [22] for object detection, the entire system can be easily and quickly (just few seconds) adapted to detect novel target objects. All the mentioned improvements result in an online robotic application that makes the robot capable of inferring where the human partner's attention is targeted while interacting

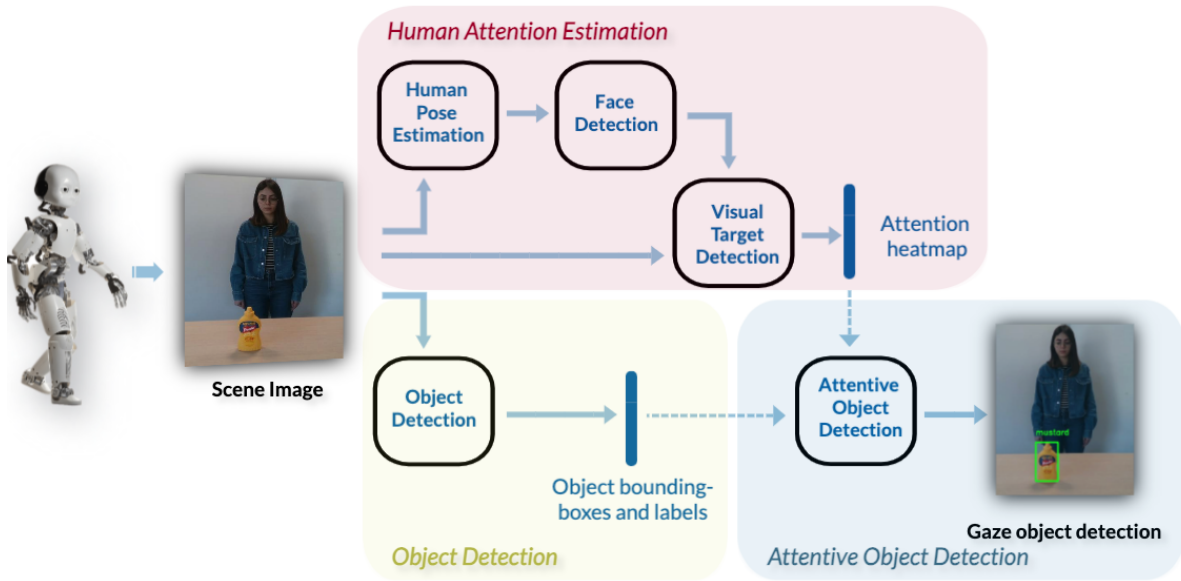


Fig. 2: Pipeline of the presented architecture. The *Human Attention Estimation* pathway produces a heatmap of the gaze target. This heatmap as well as the bounding boxes and labels from the *Object Detection* module are then used by the *Attentive Object Detection* module to predict the specific object that is visually attended by the human.

with them.

III. METHODS

The pipeline proposed in this study is made out of three major pathways as represented in Figure 2: the *Human Attention Estimation* pathway that aims at detecting the attention target of the human, the *Object Detection* pathway that recognizes and localizes the objects in the scene, and finally the *Attentive Object Detection* pathway that provides the gazed object from the human.

A. Human Attention Estimation

The *Human Attention Estimation* pathway is characterised mainly by three distinct modules: 1) Human Pose Estimation, 2) Face Detection, and 3) Visual Target Detection. Having the RGB image as input, the final output of this pathway is the real-time prediction of the attention target of the human, provided in the form of a heatmap. Figure 2 shows how the three modules are connected. In the following paragraphs we describe each of them.

Human Pose Estimation. We rely on the OpenPose architecture, proposed in [23]. Briefly, OpenPose is a system for multi-human pose estimation, that receives in input RGB frames and predicts the location in pixel (x,y) of 135 anatomical key-points of each person in the image (25 and 70 key-points for the body pose and for the face, respectively), associating also a confidence level k to each prediction. In our pipeline, we use this approach to detect the human in front of the robot.

Face Detection module. We rely on the method for face recognition presented in [15] to detect and extract the human face from image. Specifically, the face key-points extracted by the *Human Pose Estimation* are used as input for this module. The output is the bounding box that indicates the head of the person in front of the robot. Note that, in [21], they assume that the information of the face location is available, reading it from a txt file. That is a strong limit in applying the method in online robotic applications. In this work, we use the *Human Pose Estimation* jointly with the *Face Detection* to provide, online, the input to the *Visual Target Detection module*, allowing the pipeline to run on the real robot.

Visual Target Detection module. This module takes as input the RGB image from the camera of the robot and the bounding box of the face extracted by the previous module (namely, the *Face Detection*). It provides as output the heatmap representing the area in the image that are more likely to be the target of the human attention. Specifically, this is a matrix of the same dimensions of the image, where each cell corresponds to a pixel in the image. The value of each cell ranges from 0 to 1 (respectively, the lowest and the highest probability to be –or to be close to– the target of human attention). For this module, we rely on the network presented in [21]. This is composed by three main parts. The first one is called *Head Conditioning Branch* and it uses the head bounding box, encoded into a convolutional feature map (head feature map) together with the information of the location of the human’s head in the image to predict a first attention map. The second part is the *Main Scene*



Fig. 3: Sample frames extracted from the proposed *ObjectAttention* dataset, representing different participants performing the gazing task, over five sessions with different number of objects.

Branch, that multiplies the convolutional feature map of the entire image with the attention map and concatenates the result with the previously computed head feature map. The final tensor represents the input for the third and last part, namely, the *Recurrent Attention Prediction Branch*. This, firstly encodes the tensor in order to be used as input for a convolutional Long Short-Term Memory network. Then, the output of this latter is up-sampled by a decoder into the final attention heatmap. In this work, we fine-tuned the weights of the network by using our dataset and the resulting model is used for the developed application and for the experimental analysis. The details regarding the dataset and the training process are reported in Sec. IV and V-A, respectively.

B. Object detection

The *Object Detection* pathway is mainly characterized by one module that takes the RGB images from the camera of the robot as input and gives as output the bounding boxes of the objects of interest present in the scene. For doing that, we rely on the On-line object detection approach, presented in [7], [8]. This system is based on Mask R-CNN architecture conveniently adapted so that it can be re-trained online with a few seconds of training time, allowing for a fast adaptation without a performance loss. We trained the On-line object detection with data acquired using the pipeline described in [24]. More details about the training process are reported in Sec. V-A.

C. Attentive object detection

The third pathway combines all the extracted information from the human attention with the objects in the scene to detect the object that is the target of the human gaze. Specifically, it takes as input the RGB image, the heatmap from the *Visual Target Detection Module*, and all the bounding boxes

and labels predicted by the *Object Detection*. The output of this module is the bounding box and label of the attended object.

Firstly, the heatmap is processed to identify the contour of the area with the highest values which corresponds to the area of the image where the human is focusing their gaze on (the hottest part of the heatmap). Then, we compute the center of the obtained area and the surrounding bounding box. We use this information to select the object that, most likely, is the focus of human attention. Precisely, we choose the object that either presents the smallest Intersection over Union (IoU) with the bounding box of the hottest part of the heatmap or, if this latter does not intersect any object box, we select the one whose center is the closest to the center of the hottest part.

IV. DATASET

A major contribution of this work is the *ObjectAttention* dataset. We collected it with the aim of representing a human-robot collaboration in a table-top scenario. In this setting, the human partner gazes at different objects and the robot partner understands the gaze direction and the target object. In this work, we used this dataset to train and evaluate the performance of each component of the presented architecture and to validate the entire system. The dataset will be made available for reproducibility. In the next paragraphs, we present the dataset by describing the data collection and annotation processes that we performed.

A. Data collection sessions

For the data collection, we recruited a total of 10 participants, consisting of 4 females and 6 males and all of them had normal or corrected normal vision. The data collection was conducted with the iCub Humanoid robot [10], and all

participants provided written informed consent. To collect the dataset we positioned the iCub, with a RealSense 415 camera mounted on its head, on one side of a table. On the table, we placed up to five distinct objects from the YCB dataset [6] (an example of this setup is illustrated in Fig. 1). The objects were placed in various arrangements, different for all the participants. For different sessions, the participants are instructed to stand on the other side of the table facing the robot and look at the requested object in a natural and spontaneous manner. The frames were recorded using the RealSense 415 camera and the YARP middleware [25].

For the sake of diversity, we collected data in 5 different sessions for each participant, starting with one object in the scene and gradually increasing the number of objects up to five, in each session. For each session, we performed two distinct trials, with two different settings obtained keeping the same number of objects but changing the object types and their arrangements on the table. For each session, for each trial, each object is gazed at for a 5-second period by the participant and the gaze target ground truth is annotated considering the instructions given to the participant. We collect one video for each different object lasting 5 seconds.

The resulting dataset consists of 22,732 frames. When considered as a sequence there are 250 number of videos, depicting 10 participants in 2 different trials for each of the 5 sessions, gazing at the different objects. Additionally, for at least one trial in each of the sessions, we placed a distracting object (i.e., the *pringles* object) on the table, at which the participant was not asked to gaze. Example frames for three participants for different sessions are reported in Fig. 3.

Finally, one of the motivations that have driven us to collect and annotate a new dataset is the fact that the dataset used in [21] contains much more conditions in which the gaze was directed toward the upper part of the map. This is clearly visible in Fig. 4 that depicts the density maps of the gaze targets for the dataset in [21] (left) and the one we collected (right). Our dataset, in contrast, considers the situation in which the human and robot are looking at objects placed on a table. To improve performance in the considered setting, the method proposed in [21] was fine-tuned using our dataset.

B. Data annotation

For each setting, the bounding box of the participant’s head and the target object are required. The participants’ head bounding box was extracted using the key-points estimated by *Openpose* [26] and manually refined to be considered as ground truth. Furthermore, we manually annotated the bounding boxes and classes of all the objects on the table, highlighting the one that is the target of the participant’s attention. The gaze target point is chosen as the center of the gazed object. The bounding boxes labeling was done using the *LabelImg*¹ framework.

¹<https://github.com/tzutalin/labelImg>

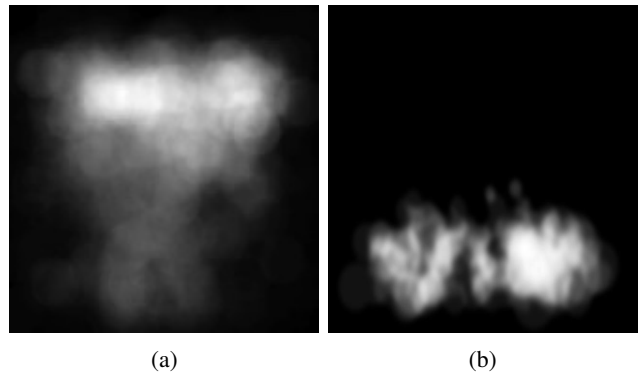


Fig. 4: Gaze target location density. (a) The density map of the gaze targets for the dataset in [21] and (b) for our dataset.

V. EXPERIMENTS

While the video submitted as supplementary material shows the functioning of the proposed application, in this section, we demonstrate its effectiveness by reporting on the experimental evaluation. Firstly, we describe how we trained some of the components of the pipeline (Sec. V-A) and the experimental conditions used for our analysis (Sec. V-B). Then, we present the obtained results, i.e., we demonstrate the improvement in using the collected data to fine-tune the *Visual Target Detection module* (sec. V-C) and we conduct experiments to evaluate the overall performance of our presented architecture (Sec. V-D and V-E).

A. Model training

In this work, two different modules have been re-trained to better fit the considered conditions, namely, the *Object Detection* and the *Visual Target Detection*.

Object Detection training. We trained the On-line object detection with data acquired using the pipeline described in [24]. Specifically, a human teacher shows the objects of interest to the robot, one at a time, holding them in their hand and moving it in front of the robot for around 30 seconds. The information from the robot’s depth sensors is used to localise the object and follow it with the robot’s gaze. The latter can be segmented and the corresponding bounding box automatically assigned and gathered as ground truth together with the object’s label, provided verbally. After each object demonstration, the collected data is used to update the current object detection model, optimizing its weights in few seconds.

Visual Target Detection fine-tuning. To fine-tune the Visual Target Detection module, we randomly split the ObjectAttention dataset by participants, considering approximately 70% of the dataset (data from 7 participants) as train set, and the remaining 30% as test set, ensuring no overlap of data between the train and test splits. We fine-tuned the spatio-temporal model of the *Visual Target Detection* on the train set performing a warm training re-start with the pre-

trained weights provided by the authors [21], and empirically choosing the hyper-parameters as follows: *learning rate* = $5e^{-5}$, *batch size*= 4, *chunk size*= 3, *number of epochs*= 10.

To ensure the statistical relevance of the presented experiments, we repeat the training and evaluation of the model for 3 times, by performing 3 different splits of the dataset as described above. We report performance in terms of mean and standard deviation for the considered metrics over all the repetitions as shown in Tab. I.

B. Experimental Setup

The performance of the *Visual Target Detection* was evaluated in terms of the *Area Under the Curve* (AUC) and *Distance* metrics. For the first metric, each cell in the spatially-discretized image is classified as either the gaze target or not. The ground truth comes from thresholding a Gaussian confidence mask centered at the human annotator’s target location. The final heatmap provides the prediction confidence score which is evaluated at different thresholds in the ROC curve. The AUC of this ROC curve is considered. The *Distance* metric, instead, is defined as the \mathbb{L}_2 distance between the annotated target location and the prediction given by the pixel of the maximum value in the heatmap, with image width and height normalized to 1.

Finally, the performance for the entire pipeline is measured as the *Accuracy* of the detected gazed objects. Specifically, for each image, we compare the bounding box of the predicted gazed object with the one of the corresponding ground truth object. If the gazed object is correctly identified, the prediction is counted as a true positive, otherwise it is predicted as a false negative.

To run the experiments, the *Human Pose Estimation* module was run on an Alienware workstation with an external NVIDIA GTX 1080TI GPU while the remaining modules were executed on another Alienware workstation with graphics NVIDIA GeForce RTX 3080 additionally equipped with an external NVIDIA GTX 2080TI GPU.

C. Fine-tuning of the Visual Target Detection module

We firstly analyze the impact of fine-tuning the *Visual Target Detection* module on our dataset. In Tab. I, we report the performance comparison of the model trained as explained in Sec. V-A (**Fine-tuning** in Tab. I) with the model presented in [21] (**Pre-trained model** in Tab. I). As it can be seen fine-tuning the model on the proposed ObjectAttention dataset allows to get better performance. Specifically, the predicted hottest point in the heat-map is closer to the true gazed point of ~ 0.04 . Note that this is a relevant difference since the Distance metric is computed on an image with width and height normalized to 1. This result is also supported by the improvement of the AUC metric of 5%. Getting a precise heat-map is crucial in order to get a better selection of the bounding box of the gazed object. This improvement is due to the fact that the model was fine-tuned using a dataset that more closely represents the target scenario (table-top). Nevertheless we show qualitatively that the fine-tuned model is still able to predict the gaze direction,

Method	AUC (%) \uparrow	\mathbb{L}_2 distance \downarrow
Pre-trained model	87.5 ± 0.9	0.131 ± 0.014
Fine-tuning	92.5 ± 1.9	0.089 ± 0.014

TABLE I: Quantitative evaluation of the *Visual Target Detection* model on the presented *ObjectAttention* dataset.

for those areas in the map that are not on the table-top and that are under-represented in our dataset (see video submitted as supplementary material). This is due to the fact that we initialized the network for our fine-tuning with the weights presented in [21], that have been trained on the VideoAttentionTarget dataset [21].

D. Accuracy evaluation of the pipeline

We study the performance of the overall pipeline presented in Sec. III evaluating it on the proposed ObjectAttention dataset. Specifically, for the *Visual Target Detection* module, we chose one of the model trained on the three dataset splits from the experiment reported in Sec. V-C and we use it in our pipeline. To get quantitative results, we consider the same test set of three participants used to previously evaluate the fine-tuned model (i.e., the three participants that have not been used for the training). However, differently from the previous section, since we need to analyze the performance of the entire pipeline of detecting the target gazed object, we will consider, as ground truth, the bounding boxes and labels of the objects on the table and of the target gazed object.

Firstly, we analyze the overall accuracy of the pipeline in detecting the gazed target object by the three different participants in the test set. Specifically, from our experiments it came out that the pipeline succeeds in detecting the right target object for the 79.5% of the times. Note that, this accuracy number represents the performance of the integration of the *Visual Target Detection*, the *Object Detection* and the *Attentive Object Detection*.

It is also possible to assess the performance of the model qualitatively by examining the video in the supporting materials. Additionally, Fig. 5 illustrates a selection of sample frames from the output, including attention heatmaps and bounding boxes, highlighting the head of the participant (detected by the *Face Detection* module) and the hottest areas of the heatmap in the frames of the top row, while the final gaze object bounding box and label are presented in the bottom row frames.

E. Performance analysis

To further study the proposed pipeline, in the next paragraphs we present the analysis of the performance of the system for different objects, sessions showing also the effect of the distractor object in the scene.

Per object performance. In Fig. 6, we report the level of accuracy achieved when the different objects are considered as target. As it can be observed, the system has a high performance for almost all the objects except for the object class *Bleach*. By analyzing the errors, we could find that

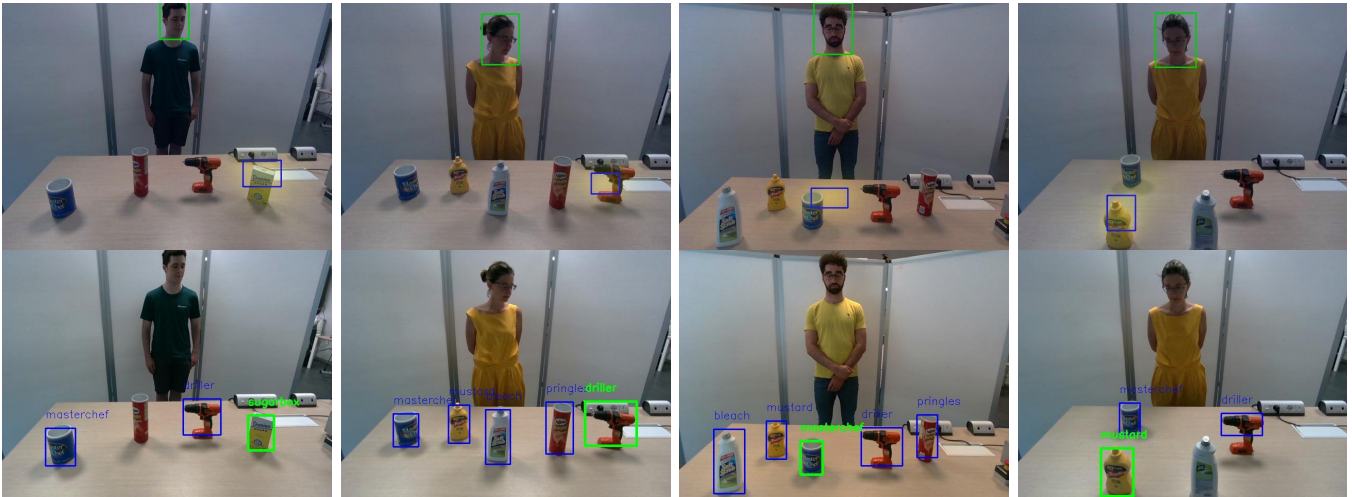


Fig. 5: Selection of sample output frames of the proposed pipeline. The first row depicts the scene image as well as the head bounding box of the participant detected by the *Face Detection* module, the attention heatmap of the participant, and the bounding box of the hottest area of the heatmap. While the second row depicts the related gaze target selections for the frames of the first row.

this is mainly due to a problem of the object detection that sometimes does not locate correctly this object in the image. This might be due to the fact that the training conditions for the detector were really different from the testing ones. Specifically, even if it proved to be effective the most of the time [24], training the detection model with handheld objects, with the pipeline proposed in [24] might cause some generalization problems due to the so called domain shift [22] between the train and the test sets. However, it has been shown in previous work [27], [22], [28] that this can be solved by, for instance, integrating (i) a robot’s autonomous exploration of the new domain and (ii) weakly-supervised learning techniques.

Per session performance. Fig. 7 depicts the accuracy levels of the overall pipeline on various sessions. As it can be observed, performance of the system slightly decreases for higher sessions. This is reasonable since, for higher sessions, the number of objects in the scene increases and thus the table becomes more cluttered. However, the accuracy level is still acceptable even with the most cluttered scenes, showing that this is not a limitation for the proposed system.

The effect of the distractor. Finally, we report on the impact of the distracting objects on the system performance. Of course, all the objects present on the table are distracting objects when the human is gazing at only one of them. However, to analyze their impact, we select one sample object (i.e., the *pringles*) as distractor in our dataset. Then, the *Object Detection* module has been trained to detect it, but the participants was not asked to gaze at it. Our aim in this experiment is to verify if the presence of the distractor object causes particular problems in identifying the correct target object. From our experiments, we find that only for the

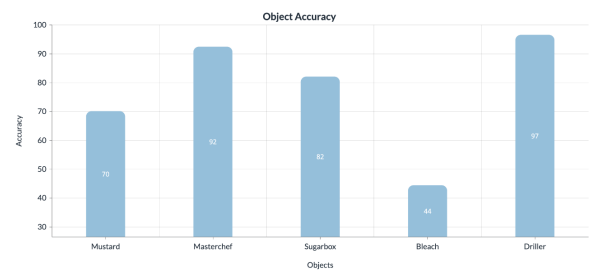


Fig. 6: Accuracy analysis on each of the objects involved in the experiments.

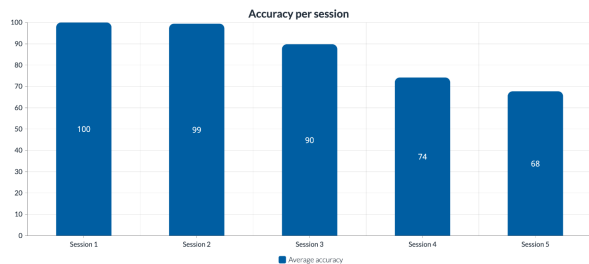


Fig. 7: Average accuracy on each of the sessions for all the participants.

~3% of the frames were the distracting object is present, this causes a mistake in the predictions, demonstrating that this is not a limitation of the proposed system.

VI. CONCLUSIONS

In this paper, we presented a novel system for detecting the focus of attention of a human in relation to the objects in the scene. Our method combines an online object detection algorithm with a network for gaze estimation conditioned

on the pose of the human, estimated using a pose estimation method. The system provides information about the objects that may capture the human's visual attention. Through the experimental analysis of our pipeline and the evaluation using a novel dataset collected with the iCub humanoid robot, we have demonstrated the effectiveness of our approach in accurately detecting the target of human attention. Our results indicate that the integration of face detection, human attention prediction, and online object detection in our pipeline enables the robot to perceive and interpret human gaze within its environment, which is a fundamental cue to establish joint attention with human partners. The developed system is promising in enhancing the robot's social awareness and responsiveness, allowing for more natural and contextually appropriate interactions in social robotics. The presented pipeline and the accompanying dataset provide a valuable resource for further research in the field of human-robot interaction and gaze detection. Future work will explore the integration of additional cues related to the object of interests, such as language, and other social cues, such as facial expressions and gestures, to further enhance the robot's understanding of human intentions and emotions.

REFERENCES

- [1] T. Allison, A. Puce, and G. McCarthy, "Social perception from visual cues: role of the sts region," *Trends in cognitive sciences*, vol. 4, no. 7, pp. 267–278, 2000.
- [2] K. A. Pelphrey, J. D. Singerman, T. Allison, and G. McCarthy, "Brain activation evoked by perception of gaze shifts: the influence of context," *Neuropsychologia*, vol. 41, no. 2, pp. 156–170, 2003.
- [3] F. Babel, J. Kraus, L. Miller, M. Kraus, N. Wagner, W. Minker, and M. Baumann, "Small talk with a robot? the impact of dialog content, talk initiative, and gaze behavior of a social robot on trust, acceptance, and proximity," *International Journal of Social Robotics*, pp. 1–14, 2021.
- [4] B. Holman, A. Anwar, A. Singh, M. Tec, J. Hart, and P. Stone, "Watch where you're going! gaze and head orientation as predictors for social robot navigation," in *2021 IEEE International Conference on Robotics and Automation (ICRA)*. IEEE, 2021, pp. 3553–3559.
- [5] U. Kurylo and J. R. Wilson, "Using human eye gaze patterns as indicators of need for assistance from a socially assistive robot," in *Social Robotics: 11th International Conference, ICSR 2019, Madrid, Spain, November 26–29, 2019, Proceedings 11*. Springer, 2019, pp. 200–210.
- [6] B. Calli, A. Singh, A. Walsman, S. Srinivasa, P. Abbeel, and A. M. Dollar, "The ycb object and model set: Towards common benchmarks for manipulation research," in *2015 international conference on advanced robotics (ICAR)*. IEEE, 2015, pp. 510–517.
- [7] F. Ceola, E. Maiettini, G. Pasquale, L. Rosasco, and L. Natale, "Fast object segmentation learning with kernel-based methods for robotics," in *2021 IEEE International Conference on Robotics and Automation (ICRA)*, 2021, pp. 13 581–13 588.
- [8] E. Maiettini, G. Pasquale, L. Rosasco, and L. Natale, "On-line object detection: a robotics challenge," *Autonomous Robots*, Nov 2019. [Online]. Available: <https://doi.org/10.1007/s10514-019-09894-9>
- [9] P. Chevalier, K. Kompatsiari, F. Ciardo, and A. Wykowska, "Examining joint attention with the use of humanoid robots—a new approach to study fundamental mechanisms of social cognition," *Psychonomic Bulletin & Review*, vol. 27, pp. 217–236, 2020.
- [10] G. Metta, L. Natale, F. Nori, G. Sandini, D. Vernon, L. Fadiga, C. von Hofsten, K. Rosander, M. Lopes, J. Santos-Victor, A. Bernardino, and L. Montesano, "The icub humanoid robot: an open-systems platform for research in cognitive development." *Neural networks : the official journal of the International Neural Network Society*, vol. 23, no. 8-9, pp. 1125–34, 1 2010.
- [11] M. Lombardi, E. Maiettini, D. De Tommaso, A. Wykowska, and L. Natale, "Toward an attentive robotic architecture: Learning-based mutual gaze estimation in human–robot interaction," *Frontiers in Robotics and AI*, vol. 9, p. 770165, 2022.
- [12] K. Krafska, A. Khosla, P. Kellnhofer, H. Kannan, S. Bhandarkar, W. Matusik, and A. Torralba, "Eye tracking for everyone," in *Proceedings of the IEEE conference on computer vision and pattern recognition*, 2016, pp. 2176–2184.
- [13] R. Athavale, L. S. Motati, and R. Kalahasty, "One eye is all you need: Lightweight ensembles for gaze estimation with single encoders," *arXiv preprint arXiv:2211.11936*, 2022.
- [14] Y. Cheng, X. Zhang, F. Lu, and Y. Sato, "Gaze estimation by exploring two-eye asymmetry," *IEEE Transactions on Image Processing*, vol. 29, pp. 5259–5272, 2020.
- [15] M. Lombardi, E. Maiettini, V. Tikhanofov, and L. Natale, "icub knows where you look: Exploiting social cues for interactive object detection learning," in *2022 IEEE-RAS 21st International Conference on Humanoid Robots (Humanoids)*, 2022, pp. 480–487.
- [16] O. Sumer, P. Gerjets, U. Trautwein, and E. Kasneci, "Attention flow: End-to-end joint attention estimation," in *Proceedings of the IEEE/CVF Winter Conference on Applications of Computer Vision*, 2020, pp. 3327–3336.
- [17] L. Fan, Y. Chen, P. Wei, W. Wang, and S.-C. Zhu, "Inferring shared attention in social scene videos," in *Proceedings of the IEEE conference on computer vision and pattern recognition*, 2018, pp. 6460–6468.
- [18] A. Recasens, C. Vondrick, A. Khosla, and A. Torralba, "Following gaze in video," in *Proceedings of the IEEE International Conference on Computer Vision*, 2017, pp. 1435–1443.
- [19] E. Chong, N. Ruiz, Y. Wang, Y. Zhang, A. Rozga, and J. M. Rehg, "Connecting gaze, scene, and attention: Generalized attention estimation via joint modeling of gaze and scene saliency," in *Proceedings of the European conference on computer vision (ECCV)*, 2018, pp. 383–398.
- [20] A. Saran, S. Majumdar, E. S. Short, A. Thomaz, and S. Niekum, "Human gaze following for human-robot interaction," in *2018 IEEE/RSJ International Conference on Intelligent Robots and Systems (IROS)*. IEEE, 2018, pp. 8615–8621.
- [21] E. Chong, Y. Wang, N. Ruiz, and J. M. Rehg, "Detecting attended visual targets in video," in *Proceedings of the IEEE/CVF conference on computer vision and pattern recognition*, 2020, pp. 5396–5406.
- [22] E. Maiettini, G. Pasquale, V. Tikhanofov, L. Rosasco, and L. Natale, "A weakly supervised strategy for learning object detection on a humanoid robot," in *2019 IEEE-RAS 19th International Conference on Humanoid Robots (Humanoids)*, 2019, pp. 194–201.
- [23] Z. Cao, G. Hidalgo, T. Simon, S.-E. Wei, and Y. Sheikh, "Openpose: realtime multi-person 2d pose estimation using part affinity fields," *IEEE transactions on pattern analysis and machine intelligence*, vol. 43, no. 1, pp. 172–186, 2019.
- [24] E. Maiettini, G. Pasquale, L. Rosasco, and L. Natale, "Interactive data collection for deep learning object detectors on humanoid robots," in *2017 IEEE-RAS 17th International Conference on Humanoid Robotics (Humanoids)*, Nov 2017, pp. 862–868.
- [25] G. Metta, P. Fitzpatrick, and L. Natale, "Yarp: Yet another robot platform," *International Journal of Advanced Robotic Systems*, vol. 3, no. 1, p. 8, 2006. [Online]. Available: <https://doi.org/10.5772/5761>
- [26] Z. Cao, T. Simon, S.-E. Wei, and Y. Sheikh, "Realtime multi-person 2d pose estimation using part affinity fields," in *Proceedings of the IEEE conference on computer vision and pattern recognition*, 2017, pp. 7291–7299.
- [27] E. Maiettini, "From constraints to opportunities: Efficient object detection learning for humanoid robots," *Ph.D. thesis, University of Genoa*, 2020.
- [28] E. Maiettini, V. Tikhanofov, and L. Natale, "Weakly-supervised object detection learning through human-robot interaction," in *2020 IEEE-RAS 20th International Conference on Humanoid Robots (Humanoids)*, 2021, pp. 392–399.